

Deep Transfer Learning Based Downlink Channel Prediction for FDD Massive MIMO Systems

Yuwen Yang, Feifei Gao, Zhimeng Zhong, Bo Ai, and Ahmed Alkhateeb,

Abstract—Artificial intelligence (AI) based downlink channel state information (CSI) prediction for frequency division duplexing (FDD) massive multiple-input multiple-output (MIMO) systems has attracted growing attention recently. However, existing works focus on the downlink CSI prediction for the users under a given environment and is hard to adapt to users in new environment especially when labeled data is limited. To address this issue, we formulate the downlink channel prediction as a deep transfer learning (DTL) problem, and propose the direct-transfer algorithm based on the fully-connected neural network architecture, where the network is trained in the manner of classical deep learning and is then fine-tuned for new environments. To further improve the transfer efficiency, we propose the meta-learning algorithm that trains the network by alternating inner-task and across-task updates and then adapts to a new environment with a small number of labeled data. Simulation results show that the direct-transfer algorithm achieves better performance than the deep learning algorithm, which implies that the transfer learning benefits the downlink channel prediction in new environments. Moreover, the meta-learning algorithm significantly outperforms the direct-transfer algorithm, which validates its effectiveness and superiority.

Index Terms—Deep transfer learning (DTL), meta-learning, few-shot learning, downlink CSI prediction, FDD, massive MIMO

I. INTRODUCTION

The acquisition of downlink channel state information (CSI) is a very challenging task for frequency division duplexing (FDD) massive multiple-input multiple-output (MIMO) systems due to the prohibitively high overheads associated with downlink training and uplink feedback [1]–[3]. By exploiting the angular and delay reciprocities between the uplink and the downlink [4]–[6], conventional methods proposed to reduce the downlink training overhead by extracting frequency-independent information from the uplink CSI, or to reduce the uplink feedback overhead by using compressive sensing based algorithms [7]–[10]. Nevertheless, the conventional methods either assume that the propagation paths are distinguishable and limited or highly rely on the sparsity of channels.

Y. Yang and F. Gao are with Institute for Artificial Intelligence Tsinghua University (THUAI), State Key Lab of Intelligent Technologies and Systems, Beijing National Research Center for Information Science and Technology (BNRist), Department of Automation, Tsinghua University, Beijing, 100084, P. R. China (email: yyw18@mails.tsinghua.edu.cn, feifeigao@ieee.org).

Z. Zhong is self-employed. He resides in China (e-mail: 17671455@qq.com).

B. Ai is with the State Key Laboratory of Rail Traffic Control and Safety, Beijing Jiaotong University, Beijing 100044, China (email: boai@bjtu.edu.cn).

A. Alkhateeb is with the School of Electrical, Computer and Energy Engineering at Arizona State University, Tempe, AZ 85287, USA (e-mail: alkhateeb@asu.edu).

Recently, artificial intelligence (AI, including machine learning and deep learning, etc.) has been recognized as a potential solution to deal with the high complexity and overheads of wireless communication system [11]–[30]. Great success has been achieved in various applications such as channel estimation [13]–[16], data detection [17], [18], CSI feedback [19]–[21], beamforming [22]–[24], and hybrid precoding [25], etc. Specifically, [15] proposed to learn the mapping from the channels of high-resolution ADC antennas to those of low-resolution ADC antennas, which achieves better performance than existing low-resolution ADC related channel prediction methods. Furthermore, AI based downlink CSI prediction for FDD systems has also been studied in many works [27]–[30]. In [27], a convolutional neural network is proposed to predict the downlink CSI from the uplink CSI for single-antenna FDD systems. Based on the CSI correlations between different base station (BS) antennas, linear and support vector based regression methods have been proposed to use the downlink CSI of partial BS antennas to predict the whole downlink CSI, which can reduce the overheads of both downlink pilots and uplink feedback [28]. In fact, [29] develops the channel mapping in space and frequent concept which proves that deep neural networks (DNNs) can learn not only the correlation between closely-located BS antennas but also between the base station arrays that are positioned at different locations or different frequency bands in the same environment. By exploiting the mapping relation between the uplink and downlink CSI in FDD massive MIMO systems, an efficient complex-valued based DNN is trained to predict the downlink CSI only from the uplink CSI, i.e., no downlink pilot is needed at all [30].

Compared with conventional methods (e.g. [7], [8]), AI aided downlink CSI prediction benefits from the excellent learning capability of DNNs and does not require accurate channel models or high computational operations. However, existing AI aided downlink CSI prediction methods [27]–[30] all focus on training models for users in a certain environment. Since users may experience different wireless transmission environments, data collection and training the models from scratch are required for the users in new environments [27]–[30]. Typically thousands of samples and training epochs are required for training one DNN, and thus training a new DNN for each user would face unacceptable time and data cost. Therefore, it is highly desirable to design a method that can adapt to new environments with a small amount of data.

Inspired by human’s capability to transfer knowledge from previous experience, transfer learning, which aims to improve the performance of target tasks by exploiting the knowledge from source tasks, becomes a promising technology in ma-

chine learning area to solve similar tasks with limited labeled data. Studies on transfer learning date back from 1995 in different names, such as incremental/cumulative learning, life-long learning, multi-task learning, and learning to learn, etc [31]. Generally, transfer learning algorithms acquire knowledge from source tasks by pre-training a model on a large-scale source dataset and then fine-tune the pre-trained model on a small-scale target dataset¹. With the rapid development of deep learning, the concept of deep transfer learning (DTL) is proposed by combining transfer learning with deep learning [33]. The methodology in transfer learning can be easily generalized to DTL, including instance-transfer, feature-representation-transfer, and parameter-transfer, etc [31]. In particular, the model-agnostic meta-learning (MAML) algorithm proposed in [34], a classical parameter-transfer learning algorithm, is known for its universal applicability and the state-of-the-art performance in few-shot learning. Unlike prior meta-learning algorithms [35]–[37] that learn an update function and impose restrictions on the model architecture, the MAML algorithm learns a model initialization that can effectively adapt to a new task with a small amount of labeled data.

In this paper, we formulate the downlink channel prediction for FDD massive MIMO systems as a DTL problem, where each learning task aims to predict the downlink CSI from the uplink CSI for users in a certain environment. We develop the *direct-transfer algorithm*, where the model is trained on the data from all previous environments using classical deep learning and is then fine-tuned with limited data from a new environment. To achieve more effective transfer, we further proposed the *meta-learning algorithm* that learns a model initialization by an alternating training procedure, consisting of the inner-task and the across-task updates. We also propose the *no-transfer algorithm* as a baseline algorithm, where the model is trained in the manner of classical deep learning and is directly tested on the data from a new environment without parameter adaption. Furthermore, theoretical analysis and complexity comparisons are presented for the proposed three algorithms. Simulation results show that the direct-transfer algorithm outperforms the no-transfer algorithm, which validates that transfer learning can effectively improve the performance of downlink channel prediction in new environments. Moreover, the meta-learning algorithm significantly outperforms the direct-transfer algorithm, which demonstrates its superiority over the direct-transfer algorithm.

The remainder of this paper is organized as follows. The system model for FDD massive MIMO systems is introduced in Section II. The DTL problem is formulated in Section III. The no-transfer and direct-transfer algorithms are presented in Section IV. The meta-learning algorithm is developed in Section V. Numerical results are given in Section VI. Our main conclusions are given in Section VII.

Notations: The bold and lowercase letters denote vectors while the bold and capital letters denote matrices. The notations $[z]_p$ and $\text{len}(z)$ denote the p -th entry and the length

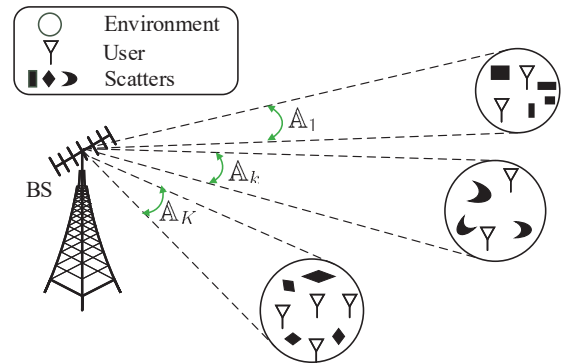


Fig. 1. Downlink CSI prediction for the FDD Massive MIMO system, i.e., a typical massive connectivity scenario [38].

of the vector \mathbf{x} , respectively. The notations $\Re[\cdot]$ and $\Im[\cdot]$, respectively, denote the real and imaginary parts of matrices, vectors or scales. The notation $\|\mathbf{x}\|_1$ denotes the L_1 norm of \mathbf{x} . The notation $(\cdot)^T$ denotes the transpose of a matrix or a vector. The notation \mathbb{R}^{2M} represents the $2M$ -dimensional real vector space. The notation \circ represents the composite mapping operation. The notation $\mathcal{N}_C(\mathbf{0}, \mathbf{I})$ represents the standard complex Gaussian distribution. The notation $E[\cdot]$ represents the expectation with respect to all random variables within the brackets. The notation \leftarrow represents the assignment operation while the notation \rightarrow represents the direction of the trajectory.

II. SYSTEM MODEL

We consider an FDD massive MIMO system, where BS is equipped with $M \gg 1$ antennas in the form of uniform linear array (ULA)² and serves multiple single-antenna users, as shown in Fig. 1. The users are randomly distributed in K regions and users in the same region share the same propagation environment. Denote \mathbb{B}_k as the set of users in the k -th region. Then, the channel between the u -th ($u \in \mathbb{B}_k$) user and BS can be expressed as [8]:

$$\begin{aligned} \mathbf{h}_u(f) &= \int_{\theta \in \mathbb{A}_k} \alpha_u(\theta) \mathbf{a}(\theta) d\theta \\ &= \int_{\bar{\vartheta}_k^-}^{\bar{\vartheta}_k^+} |\alpha_u(\theta)| e^{-j2\pi f \tau_u(\theta) + j\phi_u(\theta)} \mathbf{a}(\theta) d\theta, \end{aligned} \quad (1)$$

where f is the carrier frequency of the u -th user, while $|\alpha_u(\theta)|$, $\phi_u(\theta)$ and $\tau_u(\theta)$ are the attenuation amplitude, the phase shift and the delay of the incident signal ray coming from direction of arrival (DOA) θ , respectively. Meanwhile, $\mathbb{A}_k \triangleq [\bar{\vartheta}_k^-, \bar{\vartheta}_k^+]$ is the incident angle spread (AS) of the users in the k -th region with $\bar{\vartheta}_k^-$ and $\bar{\vartheta}_k^+$ being the corresponding lower and upper bounds of AS. The incident AS is assumed to be limited in a narrow region due to the limited local scattering

¹In unsupervised learning [32], labeled data in target tasks are not required. Unsupervised learning algorithms require strong assumptions of data distributions and are hard to be generalized to different problems, and therefore will not be discussed here.

²We adopt the ULA model here for simpler illustration, nevertheless, the proposed approach does not restrict to the specific array shape, and therefore is applicable for array with arbitrary geometry.

effects at the BS side [4]–[6]. Moreover, $\mathbf{a}(\theta)$ is the the array manifold vector defined as

$$\mathbf{a}(\theta) = \left[1, e^{-j\varpi \sin \theta}, \dots, e^{-j\varpi(M-1) \sin \theta} \right]^T, \quad (2)$$

where $\varpi = 2\pi df/c$, d is the antenna spacing, and c represents the speed of light.

III. FORMULATION OF DTL PROBLEM

In this section, we first prove the feasibility of applying deep learning to predict the downlink CSI from uplink CSI for a single user. Then, we formulate the downlink channel prediction as a DTL problem and analyze the related transfer learning algorithms.

A. Deep Learning for Uplink-to-Downlink Mapping

Since the downlink and the uplink of a certain user share common physical paths and similar spatial propagation characteristics, there exists a deterministic mapping between the downlink and the uplink channels when the position-to-channel mapping is bijective (see more details referring to [29], [30]). Denote $f_{U,u}$ and $f_{D,u}$ as the uplink and the downlink frequencies of the u -th user, respectively. Then, the uplink-to-downlink mapping function can be written as

$$\Psi_{f_{U,u} \rightarrow f_{D,u}} : \{\mathbf{h}_u(f_{U,u})\} \rightarrow \{\mathbf{h}_u(f_{D,u})\}. \quad (3)$$

Although the mapping function $\Psi_{f_{U,u} \rightarrow f_{D,u}}$ cannot be described by known mathematical tools, it can be approximated by deep neural networks as shown in the following.

Let us consider the simplest three-layers fully-connected neural network (FNN) with only one input layer, one hidden layer with N neurons, and one output layer. Denote \mathbf{x} and Ω as the input data and the network parameter of FNN, respectively. Then the corresponding output can be expressed as $\text{NET}_N(\mathbf{x}, \Omega)$. Since deep learning algorithms work in real domain, we introduce the isomorphism between the complex and real domains as

$$\xi : \mathbf{z} \rightarrow (\Re(\mathbf{z}^T), \Im(\mathbf{z}^T))^T. \quad (4)$$

Denote the inverse mapping of ξ as ξ^{-1} that can be given as $\xi^{-1} : (\Re(\mathbf{z}^T), \Im(\mathbf{z}^T))^T \rightarrow \mathbf{z}$. Based on the universal approximation theorem [39], we obtain the following proposition:

Proposition 1: For any given error $\varepsilon > 0$, there exists a positive constant N large enough that satisfies

$$\sup_{\mathbf{x} \in \mathbb{H}} \|\text{NET}_N(\mathbf{x}, \Omega) - \Psi_{\xi, u, U \rightarrow D}(\mathbf{x})\| \leq \varepsilon, \quad \mathbb{H} = \{\xi \circ \mathbf{h}_u(f_{U,u})\} \subseteq \mathbb{R}^{2M}, \quad (5)$$

with $\Psi_{\xi, u, U \rightarrow D}(\mathbf{x}) = \xi \circ \Psi_{f_{U,u} \rightarrow f_{D,u}} \circ \xi^{-1}(\mathbf{x})$.

Proof. (i) Since $\forall \mathbf{x} \in \mathbb{H}$, $|\mathbf{x}| = |\mathbf{h}_u(f_{U,u})| \leq \sqrt{M}\vartheta_u |\alpha_u(\theta)|$, we know \mathbf{x} is bounded. Therefore, \mathbb{H} is a compact set; (ii) Since $\Psi_{f_{U,u} \rightarrow f_{D,u}}$ and ξ are continuous mapping and composition of continuous mappings is still a continuous mapping, we know $\Psi_{\xi, u, U \rightarrow D}(\mathbf{x})$ is a continuous function for $\forall \mathbf{x} \in \mathbb{H}$. Therefore, the i -th element of $\Psi_{\xi, u, U \rightarrow D}(\mathbf{x})$, denoted by $[\Psi_{\xi, u, U \rightarrow D}(\mathbf{x})]_i$, is also a continuous function of \mathbf{x} . Based on (i), (ii) and universal approximation theorem [39, Theorem

1], we know for any $\varepsilon_i > 0$, there exists a positive constant N_i such that

$$\sup_{\mathbf{x} \in \mathbb{H}} |\text{NET}_{N_i}(\mathbf{x}, \Omega_i) - [\Psi_{\xi, u, U \rightarrow D}(\mathbf{x})]_i| \leq \varepsilon_i, \quad (6)$$

where $\text{NET}_{N_i}(\mathbf{x}, \Omega_i)$ is the output of the network with only one neuron in the output layer, and Ω_i denotes the corresponding network parameters. By stacking $2M$ of the above networks together, we can construct a larger network $\text{NET}_N(\mathbf{x}, \Omega)$ with $N = \sum_{i=1}^{2M} N_i$, where Ω denotes the corresponding network parameters. By choosing $\varepsilon_i = \varepsilon/\sqrt{2M}$, Eq. (5) can be proved. \square

Proposition 1 reveals that the uplink-to-downlink mapping function can be approximated arbitrarily well by an FNN with a single hidden layer. It should be mentioned that although the network proposed in this work cannot obtain arbitrarily high prediction accuracy due to inadequate learning or insufficient number of hidden units [39], *Proposition 1* still provides theoretical foundation for the application of deep neural networks.

B. Definitions of DTL

For the users in the k -th environment (region), let \mathcal{X}_k and \mathcal{Y}_k denote the space³ of the uplink and the downlink channels, respectively. Then, the definitions of the “domain” and the “task” are given in the following two definitions:

Definition 1: The “domain” $\mathcal{D}(k)$ is composed of the feature space \mathcal{X}_k and the marginal probability distribution $P(\mathbf{h}_u(f_{U,u})|_{u \in \mathbb{B}_k})$, i.e., $\mathcal{D}(k) = \{\mathcal{X}_k, P(\mathbf{h}_u(f_{U,u})|_{u \in \mathbb{B}_k})\}$.

Definition 2: Define the “task” $\mathcal{T}(k)$ as the prediction of the downlink channels from the uplink channels for the users in the k -th environment. Given the specific domain $\mathcal{D}(k)$, the “task” $\mathcal{T}(k)$ is composed of the label space \mathcal{Y}_k and the prediction function \mathcal{F}_k , i.e., $\mathcal{T}(k) = \{\mathcal{Y}_k, \mathcal{F}_k\}$.

Remark 1: The prediction function \mathcal{F}_k can be learned from the training data of the k -th environment and then be used to predict the downlink channels for the users in the k -th environment. Based on the analysis in Section III-A, the prediction function \mathcal{F}_k can be interpreted as the fitting function for all the uplink-to-downlink mapping functions defined in the k -th environment, i.e., $\{\Psi_{f_{U,u} \rightarrow f_{D,u}}\}_{u \in \mathbb{B}_k}$. The prediction function \mathcal{F}_k can also be interpreted as the conditional probability distribution $P(\mathbf{h}_u(f_{D,u})|\mathbf{h}_u(f_{U,u})|_{u \in \mathbb{B}_k})$ from probabilistic view.

Classical transfer learning consists of two aspects, namely, the source domain transfer and the target domain adaption. Based on [31], the definition of transfer learning can be given as following:

Definition 3: Given the source task \mathcal{T}_S , the source domain \mathcal{D}_S , the target task \mathcal{T}_T , and the target domain \mathcal{D}_T , the aim of transfer learning is to improve the performance of the target task \mathcal{T}_T by using the knowledge from \mathcal{T}_S and \mathcal{D}_S , where $\mathcal{D}_T \neq \mathcal{D}_S$ or $\mathcal{T}_T \neq \mathcal{T}_S$.

Here we extend the single-source domain transfer to the multi-source domain transfer. Then, a more generalized definition of transfer learning can be provided as follows:

³ The space of the uplink channels is \mathcal{X} means that any possible uplink channel vector belongs to \mathcal{X} , i.e. $\mathbf{h}_u(f_{U,u}) \in \mathcal{X}$ holds for any possible u or $f_{U,u}$.

Definition 4: Given the number of source tasks K_s , the source tasks $\{\mathcal{T}_S(k)\}_{k=1}^{K_s}$, the source domains $\{\mathcal{D}_S(k)\}_{k=1}^{K_s}$, the target task \mathcal{T}_T , and the target domain \mathcal{D}_T , the aim of transfer learning is to improve the performance of the target task \mathcal{T}_T by using the knowledge from $\{\mathcal{T}_S(k)\}_{k=1}^{K_s}$ and $\{\mathcal{D}_S(k)\}_{k=1}^{K_s}$, where $\mathcal{D}_T \neq \mathcal{D}_S(k)$ or $\mathcal{T}_T \neq \mathcal{T}_S(k)$ holds for $k = 1, \dots, K_s$.

In *Definition 4*, the condition $\mathcal{D}_T \neq \mathcal{D}_S(k)$ means that either the corresponding feature space $\mathcal{X}_T \neq \mathcal{X}_S(k)$ holds or the corresponding marginal probability distribution $P_T(\mathbf{h}_u(f_{U,u}))|_{u \in \mathbb{B}_T} \neq P_{S(k)}(\mathbf{h}_u(f_{U,u}))|_{u \in \mathbb{B}_k}$ holds, where \mathbb{B}_T is the set of users in the target environment. The condition $\mathcal{T}_T \neq \mathcal{T}_S(k)$ means that either the label space $\mathcal{Y}_T \neq \mathcal{Y}_S(k)$ holds or the corresponding conditional probability distribution $P_T(\mathbf{h}_u(f_{D,u})|\mathbf{h}_u(f_{U,u}))|_{u \in \mathbb{B}_T} \neq P_{S(k)}(\mathbf{h}_u(f_{D,u})|\mathbf{h}_u(f_{U,u}))|_{u \in \mathbb{B}_k}$ holds. Since the conditional probability distributions for different prediction tasks are different, the condition $\mathcal{T}_T \neq \mathcal{T}_S(k)$ is satisfied. Therefore, the downlink channel prediction for massive MIMO systems can be formulated as a transfer learning problem.

DTL is to transfer knowledge by deep neural networks, which is defined as follows [33]:

Definition 5: Given a transfer learning task described by $\langle \{\mathcal{T}_S(k)\}_{k=1}^{K_s}, \{\mathcal{D}_S(k)\}_{k=1}^{K_s}, \mathcal{T}_T, \mathcal{D}_T \rangle$, it is a DTL task when the prediction function \mathcal{F}_T of \mathcal{T}_T is a non-linear function that is approximated by a deep neural network.

Based on *Definition 4* and *Definition 5*, the downlink channel prediction for massive MIMO systems can be formulated as a typical DTL problem, where the k -th learning task is to predict the downlink channel $\mathbf{h}_u(f_{D,u})$ from the uplink channel $\mathbf{h}_u(f_{U,u})$ for the users in the k -th environment.

C. Motivation of Meta-learning

Before resorting to DTL methods, we should first consider the question “whether to transfer”. In fact, if the source and target tasks are highly related, a deep neural network would perform well, without the need for fine-tuning the neural network based on the target environment, thanks to its remarkable generalization capability. Therefore, a classical deep learning algorithm should be considered as a baseline algorithm to investigate the necessity of transfer learning.

The second question is “how to transfer”. One natural solution is to directly use all the labeled data in the source tasks to train the network, and then fine-tune the network with the labeled data in the target task. However, the direct transfer method tends to overfit when the number of labeled data in the target task is small, as will be verified by simulations in Section VI. To overcome this challenge, and motivated by the state-of-the-art performance of the model-agnostic meta-learning algorithm in few-shot learning [34], we will propose the meta-learning algorithm based downlink channel prediction in Section V.

IV. NO-TRANSFER AND DIRECT-TRANSFER ALGORITHMS

Based on the analysis in Section III-C, we propose the no-transfer algorithm based on classical deep learning algorithms to investigate the necessity of transfer learning. Then, the

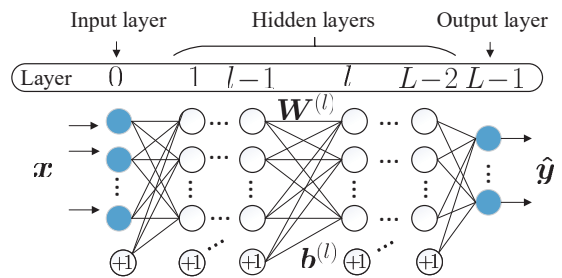


Fig. 2. The FNN architecture, where the circles labeled with “+” represent the bias units, blank circles represent the units in the hidden layers, and blue circles represent the units in the input and the output layers.

direct-transfer algorithm is proposed and used as the benchmark of the meta-learning algorithm. Both the no-transfer and the direct-transfer algorithms adopt the FNN architecture as described in the following subsection.

A. Network Architecture

The FNN architecture has L layers, including one input layer, $L - 2$ hidden layers, and one output layer, as shown in Fig. 2. The input of FNN is $\mathbf{x} = \boldsymbol{\xi} \circ \mathbf{h}_u(f_{U,u})$. The output of the network is a cascade of nonlinear transformation of \mathbf{x} , i.e.,

$$\hat{\mathbf{y}} = \text{Net}(\mathbf{x}, \boldsymbol{\Omega}) = \mathbf{f}^{(L-1)} \circ \mathbf{f}^{(L-2)} \circ \dots \circ \mathbf{f}^{(1)}(\mathbf{x}), \quad (7)$$

where $\boldsymbol{\Omega} \triangleq \{\mathbf{W}^{(l)}, \mathbf{b}^{(l)}\}_{l=1}^{L-1}$ is the network parameters to be trained. Moreover, $\mathbf{f}^{(l)}$ is the nonlinear transformation function of the l -th layer and can be written as,

$$\mathbf{f}^{(l)}(\mathbf{x}) = \mathbf{r}^{(l)}\left(\mathbf{W}^{(l)}\mathbf{x} + \mathbf{b}^{(l)}\right), \quad 1 \leq l \leq L-1, \quad (8)$$

where $\mathbf{W}^{(l)}$ is the weight matrix associated with the $(l-1)$ -th and the l -th layers, while $\mathbf{b}^{(l)}$ and $\mathbf{r}^{(l)}$ are the bias vector and the activation function of the l -th layer, respectively. The activation function for the hidden layers is selected as the rectified linear unit (ReLU) function $[\mathbf{r}_{\text{re}}(\mathbf{z})]_p = \max\{0, [\mathbf{z}]_p\}$ with $p = 1, 2, \dots, \text{len}(\mathbf{z})$. The activation function for the output layer is the linear function, i.e., $\mathbf{r}_{\text{li}}(\mathbf{z}) = \mathbf{z}$. The loss function can be written as follow:

$$\text{Loss}_{\mathbb{D}}(\boldsymbol{\Omega}) = \frac{1}{V} \sum_{v=0}^{V-1} \left\| \hat{\mathbf{y}}^{(v)} - \mathbf{y}^{(v)} \right\|_2^2, \quad (9)$$

where $\mathbf{y} = \boldsymbol{\xi} \circ \mathbf{h}_u(f_{D,u})$ is the supervise label, V is the batch size⁴, the superscript (v) denotes the index of the v -th training sample, $\mathbb{D} = \{(\mathbf{x}^{(v)}, \mathbf{y}^{(v)})\}_{v=1}^V$ is the training data of one batch, and $\|\cdot\|_2$ denotes the L_2 norm.

B. Definitions and Generation of Datasets

As mentioned in *Definition 2*, each task represents the prediction of downlink channel from the uplink channel for the users in a certain environment. In the k -th environment, U different users are involved in the generation of datasets. Denote Δf as the frequency difference between the uplink and

⁴Batch size is the number of samples in one training batch.

the downlink. Then, each uplink frequency corresponds to a certain downlink frequency, i.e., $f_{D,u} = f_{U,u} + \Delta f$. Denote the training dataset of the k -th source task as $\mathbb{D}_{\text{Tr}}(k)$. We can collect N_{Tr} sample pairs $\{(\boldsymbol{\xi} \circ \mathbf{h}_u(f_{U,u}), \boldsymbol{\xi} \circ \mathbf{h}_u(f_{D,u}))\}$ as the dataset $\mathbb{D}_{\text{Tr}}(k)$ by randomly selecting multiple uplink frequencies for users in the k -th environment.

Denote the adaption and testing datasets of the k -th target task as $\mathbb{D}_{\text{Ad}}(k)$ and $\mathbb{D}_{\text{Te}}(k)$, respectively. Similarly, the datasets $\mathbb{D}_{\text{Ad}}(k)$ and $\mathbb{D}_{\text{Te}}(k)$ can be obtained by separately collecting N_{Ad} and N_{Te} sample pairs for the k -th target task. Note that $\mathbb{D}_{\text{Ad}}(k) \cap \mathbb{D}_{\text{Te}}(k) = \emptyset$ should be satisfied to ensure the testing dataset not known to the networks.

C. No-Transfer Algorithm

The no-transfer algorithm regards the DTL problem as one classical deep learning problem, including the training and the testing stages.

In the training stage, the datasets $\{\mathbb{D}_{\text{Tr}}(k)\}_{k=1}^{K_S}$ for K_S source tasks are collected as a complete training dataset \mathbb{D}_{STr} . In each time step, V training samples are randomly selected from \mathbb{D}_{STr} as the training batch \mathbb{D}_{STrB} . Then, we employ the adaptive moment estimation (ADAM) algorithm [40] to minimize the loss function on \mathbb{D}_{STrB} , i.e., $\text{Loss}_{\mathbb{D}_{\text{STrB}}}(\boldsymbol{\Omega})$. Instead of using the gradient of the current step to guide the updates, ADAM adopts moments of the gradient to determine the direction of the optimization, which can accelerate the training, especially in the case of high curvature or noisy gradients [41, chapter 8]. By iteratively executing the ADAM algorithm on the dataset \mathbb{D}_{STr} until $\text{Loss}_{\mathbb{D}_{\text{STrB}}}(\boldsymbol{\Omega})$ converges, we can obtain the trained network parameter $\boldsymbol{\Omega}_{\text{Nt}}$.

In the testing stage, the network parameter $\boldsymbol{\Omega}_{\text{Nt}}$ is fixed. The testing datasets $\{\mathbb{D}_{\text{Te}}(k)\}_{k=1}^{K_T}$ of K_T target tasks are generated and are used to test the performance of the no-transfer algorithm. Denote $\hat{\mathbf{h}}_{\text{D}} = \boldsymbol{\xi}^{-1} \circ \hat{\mathbf{y}}$ and $\mathbf{h}_{\text{D}} = \boldsymbol{\xi}^{-1} \circ \mathbf{y}$ as the estimated and the true downlink channel, respectively. Normalized mean-squared-error (NMSE) is used to measure the prediction accuracy, which is defined as

$$\text{NMSE} = E \left[\left\| \mathbf{h}_{\text{D}} - \hat{\mathbf{h}}_{\text{D}} \right\|_2^2 / \left\| \mathbf{h}_{\text{D}} \right\|_2^2 \right]. \quad (10)$$

Denote the prediction NMSE of the no-transfer algorithm as NMSE_{Nt} that can be calculated by averaging the NMSEs of the no-transfer algorithm evaluated on K_T target environments, i.e., $\text{NMSE}_{\text{Nt}} = \sum_{k=1}^{K_T} \text{NMSE}_{\text{Nt}}(k) / K_T$, where $\text{NMSE}_{\text{Nt}}(k)$ is the NMSE evaluated on the k -th target environment. The concrete steps of the no-transfer algorithm are given in the **Algorithm 1**.

D. Direct-transfer Algorithm

In the training stage, the direct-transfer algorithm trains the network via the ADAM algorithm on the training dataset \mathbb{D}_{STr} until $\text{Loss}_{\mathbb{D}_{\text{STrB}}}(\boldsymbol{\Omega})$ converges. During the training, the network tries to learn a generalized parameter to predict the downlink CSI for users in different environments. After the training finished, the network has learned the parameter $\boldsymbol{\Omega}_{\text{Nt}}$ from the K_S source tasks. Then, the datasets $\{\mathbb{D}_{\text{Ad}}(k)\}_{k=1}^{K_T}$ and $\{\mathbb{D}_{\text{Te}}(k)\}_{k=1}^{K_T}$ of K_T target tasks are generated following

Algorithm 1: No-transfer algorithm for downlink CSI prediction

Input: Source tasks: $\{\mathcal{T}_S(k)\}_{k=1}^{K_S}$, Target tasks:

$\{\mathcal{T}_T(k)\}_{k=1}^{K_T}$, learning rate: γ , batch size: V

Output: Trained network parameter: $\boldsymbol{\Omega}_{\text{Nt}} \leftarrow \boldsymbol{\Omega}$, predicted downlink CSI based on $\{\mathbb{D}_{\text{Te}}(k)\}_{k=1}^{K_T}$, NMSE of the no-transfer algorithm: NMSE_{Nt}

```

1 Training stage
2 Randomly initialize the network parameters  $\boldsymbol{\Omega}$ 
3 Generate the training dataset  $\mathbb{D}_{\text{STr}} \triangleq \{\mathbb{D}_{\text{Tr}}(k)\}_{k=1}^{K_S}$  for  $K_S$ 
  source tasks
4 for  $t = 1, \dots$  do
5   Randomly select  $V$  training samples from  $\mathbb{D}_{\text{STr}}$  as the
   training batch  $\mathbb{D}_{\text{STrB}}$ 
6   Update  $\boldsymbol{\Omega}$  by using the ADAM algorithm (learning
   rate  $\gamma$ ) to minimize  $\text{Loss}_{\mathbb{D}_{\text{STrB}}}(\boldsymbol{\Omega})$ 
7 end
8 Testing stage
9 Initialize NMSE:  $\text{NMSE}_{\text{Nt}} \leftarrow 0$ 
10 for  $k = 1, \dots, K_T$  do
11   Generate the testing dataset  $\mathbb{D}_{\text{Te}}(k)$  for  $\mathcal{T}_T(k)$ 
12   Predict the downlink CSI base on  $\mathbb{D}_{\text{Te}}(k)$  and  $\boldsymbol{\Omega}$ 
   using Eq. (7)
13   Calculate  $\text{NMSE}_{\text{Nt}}(k)$  using Eq. (10)
14    $\text{NMSE}_{\text{Nt}} \leftarrow \text{NMSE}_{\text{Nt}} + \text{NMSE}_{\text{Nt}}(k) / K_T$ 
15 end

```

Section IV-B. For the k -th target task, the direct-transfer algorithm initializes the target-task-specific parameter $\boldsymbol{\Omega}_{T,k}$ as the trained network parameter $\boldsymbol{\Omega}_{\text{Nt}}$, then fine-tunes $\boldsymbol{\Omega}_{T,k}$ on the adaption dataset $\mathbb{D}_{\text{Ad}}(k)$ via G_{Ad} steps of ADAM updates. After the fine-tuning finished, the target-task-specific parameter $\boldsymbol{\Omega}_{T,k}$ will be fixed. Let $\text{NMSE}_{\text{Dt}}(k)$ represent the NMSE of the direct-transfer algorithm evaluated on the k -th target environment that can be obtained by testing the network on the dataset $\mathbb{D}_{\text{Te}}(k)$ using Eqs. (7) and (10). Then, the prediction NMSE of the direct-transfer algorithm can be obtained by $\text{NMSE}_{\text{Dt}} = \sum_{k=1}^{K_T} \text{NMSE}_{\text{Dt}}(k) / K_T$. The concrete steps of the direct-transfer algorithm are given in the **Algorithm 2**.

Notice that the direct-transfer algorithm utilizes the trained network parameter $\boldsymbol{\Omega}_{\text{Nt}}$ as the initialization of the direct-adaption stage for every target task. By contrast, another way is to utilize previous target-task-specific parameter $\boldsymbol{\Omega}_{T,k-1}$ as the initialization of the direct-adaption stage for the k -th target task since $\boldsymbol{\Omega}_{T,k-1}$ appears to contain the information in all the source environments and $k-1$ target environments, and therefore could enhance the performance of the algorithm. However, the real situation is that a good initialization in DTL is not to train the network parameter with as much data as possible, but to find such a parameter that can easily adapt to any target task. In a way, a good initial parameter can be interpreted as a parameter point in the parameter space that is near (or easy to get) to the optimal parameter point for most target tasks. Fig. 3 illustrates the trajectory of parameter updating during the training and direct-adaption stages of the direct-transfer algorithm. The black solid line represents the

Algorithm 2: Direct-transfer algorithm for downlink CSI prediction

Input: Source tasks: $\{\mathcal{T}_S(k)\}_{k=1}^{K_S}$, Target tasks: $\{\mathcal{T}_T(k)\}_{k=1}^{K_T}$, learning rate: β , batch size: V , number of gradsteps for adaption: G_{Ad}
Output: Trained network parameter: Ω_{Nt} , predicted downlink CSI based on $\{\mathbb{D}_{Te}(k)\}_{k=1}^{K_T}$, NMSE of the direct-transfer algorithm: $NMSE_{Dt}$

Training stage

Implement the **Algorithm 1** and obtain the trained network parameter Ω_{Nt}

Direct-adaption and Testing

Initialize NMSE: $NMSE_{Dt} \leftarrow 0$

for $k = 1, \dots, K_T$ **do**

 Generate the datasets $\mathbb{D}_{Ad}(k)$ and $\mathbb{D}_{Te}(k)$ for $\mathcal{T}_T(k)$

 Direct-adaption stage

 Load the network parameter $\Omega_{T,k} \leftarrow \Omega_{Nt}$

for $g = 1, \dots, G_{Ad}$ **do**

 Update $\Omega_{T,k}$ by using ADAM (learning rate β) to

 minimize $\text{Loss}_{\mathbb{D}_{Ad}(k)}(\Omega_{T,k})$

end

 Testing stage

 Predict the downlink CSI base on $\mathbb{D}_{Te}(k)$ and $\Omega_{T,k}$ using Eq. (7)

 Calculate $NMSE_{Dt}(k)$ using Eq. (10)

$NMSE_{Dt} \leftarrow NMSE_{Dt} + NMSE_{Dt}(k)/K_T$

end

updating trajectory of the network parameter Ω during the training stage. The blue dashed lines represent the updating trajectories of the target-task-specific parameters $\{\Omega_{T,k}\}_{k=1}^3$ during the direct-adaption stage following **Algorithm 2**. The red dash-dotted lines represent the parameter adaption process with previous target-task-specific parameter as the initial parameter. As shown in Fig. 3, the trajectory of red dash-dotted lines, i.e., $\Omega_{Nt} \rightarrow \Omega_{T,1} \rightarrow \Omega_{T,2} \rightarrow \Omega_{T,3}$, is longer than the trajectory of blue dashed lines, i.e., $\{\Omega_{Nt} \rightarrow \Omega_{T,k}\}_{k=1}^3$, which indicates Ω_{Nt} is a better initialization than $\Omega_{T,k-1}$. The intrinsic reason is that Ω_{Nt} is obtained by training the network on a large-scale and shuffled dataset, i.e., \mathbb{D}_{STr} , which has more stronger representativeness of different tasks than the small-scale adaption dataset $\mathbb{D}_{Ad}(k)$. In fact, the fine-tuning on the adaption dataset $\mathbb{D}_{Ad}(k)$ renders the network parameter away from the generalized parameter Ω_{Nt} and gets closed to the task-specific parameter $\Omega_{T,k}$.

Remark 2: It should be emphasized that parameter initialization is one of the most crucial tasks in deep learning, especially in DTL. A high-quality initialization can effectively prevent the training from getting stuck in a low-performance local minimum and thus accelerates the convergence [42], [43].

V. META-LEARNING ALGORITHM

The proposed meta-learning algorithm also adopts the FNN architecture in Section IV-A and has three stages, namely, the meta-training, the meta-adaption and the testing stages.

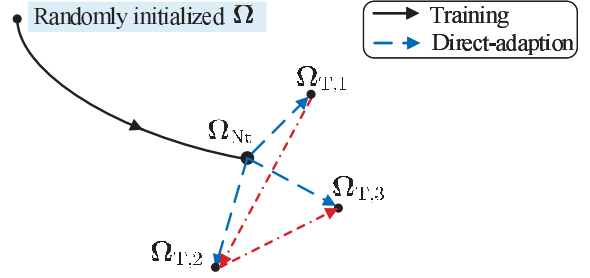


Fig. 3. Illustration of the direct-transfer algorithm, where $K_T = 3$.

A. Definitions and Generation of Datasets

For the k -th source task, two datasets should be obtained for the meta-training stage, i.e., the training support dataset $\mathbb{D}_{TrSup}(k)$ and the training query dataset $\mathbb{D}_{TrQue}(k)$. Following Section IV-B, we can collect multiple sample pairs for each source task and then randomly divide these sample pairs, i.e., $\{(\xi \circ h_u(f_{U,u}), \xi \circ h_u(f_{D,u}))\}$, into the training support dataset $\mathbb{D}_{TrSup}(k)$ and the training query dataset $\mathbb{D}_{TrQue}(k)$. Note that $\mathbb{D}_{TrSup}(k) \cap \mathbb{D}_{TrQue}(k) = \emptyset$ should be satisfied to improve the generalization capability of the network. For the k -th target task, the adaption dataset $\mathbb{D}_{Ad}(k)$ and the testing dataset $\mathbb{D}_{Te}(k)$ can be obtained following Section IV-B.

B. Meta-training Stage

In the meta-training stage, the meta-learning algorithm aims to learn a network initialization that can effectively adapt to a new task. The parameter of FNN, i.e., Ω , is randomly initialized and is then updated by two iterative processes, i.e., the inner-task and the across-task updates.

1) *Inner-task update:* Denote the source-task-specific parameter as $\Omega_{S,k}$. The goal of the inner-task updates is to minimize the loss function on the training support dataset $\mathbb{D}_{TrSup}(k)$, i.e., $\text{Loss}_{\mathbb{D}_{TrSup}(k)}(\Omega_{S,k})$, by iteratively updating the parameter $\Omega_{S,k}$. Specifically, $\Omega_{S,k}$ is initialized as the current network parameter Ω , and is then updated with G_{Tr} steps of gradient descents, i.e.,

$$\Omega_{S,k} \leftarrow \Omega_{S,k} - \beta \nabla_{\Omega_{S,k}} \text{Loss}_{\mathbb{D}_{TrSup}(k)}(\Omega_{S,k}), \quad (11)$$

where β is the inner-task learning rate.

2) *Across-task update:* In the t -th time step, we randomly select K_B source tasks out of K_S source tasks⁵ and generate corresponding support datasets $\{\mathbb{D}_{TrSup}(k)\}_{k=1}^{K_B}$ and query datasets $\{\mathbb{D}_{TrQue}(k)\}_{k=1}^{K_B}$ following Section V-A. The optimization objective of the t -th update is the loss function associated with the K_B training query datasets $\{\mathbb{D}_{TrQue}(k)\}_{k=1}^{K_B}$ and the meta-trained source-task-specific parameter $\Omega_{S,k}$, i.e.,

$$\sum_{k=1}^{K_B} \text{Loss}_{\mathbb{D}_{TrQue}(k)}(\Omega_{S,k}).$$

The network parameter Ω is updated via the ADAM algorithm with learning rate γ . After the across-task updates finished, the meta-trained network parameter will be obtained by $\Omega_{Mt} \leftarrow$

⁵Typically, there is $K_B \ll K_S$.

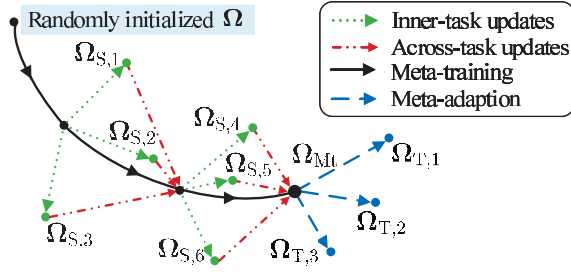


Fig. 4. Illustration of the meta-learning algorithm, where $K_B = K_T = 3$.

Ω . By alternately implementing the inner-task and across-task updates until the loss converges, the network learns model initialization that can adapt to a new task using only a small number of samples.

There are two important differences between the inner-task and across-task updates. (i) Each inner-task update is performed on the support dataset of one source task while each across-task update is performed on the query datasets of K_B source tasks; (ii) The aim of inner-task updates is to optimize the task-specific parameters $\{\Omega_{S,k}\}_{k=1}^{K_B}$ while the aim of across-task updates is to optimize the overall network parameters Ω .

C. Meta-adaption and Testing Stages

Following Section V-A, we generate the adaption datasets $\{\mathbb{D}_{Ad}(k)\}_{k=1}^{K_T}$ and the testing datasets $\{\mathbb{D}_{Te}(k)\}_{k=1}^{K_T}$ for the meta-adaption and testing stages, respectively. In the meta-adaption stage, the meta-learning algorithm aims to fine-tune the network on the adaption dataset $\mathbb{D}_{Ad}(k)$ so that the network can predict the downlink CSI on $\mathbb{D}_{Te}(k)$ as accurate as possible. For the k -th target task, the direct-transfer algorithm initializes the target-task-specific parameter $\Omega_{T,k}$ as the meta-trained network parameter Ω_{Mt} , and then fine-tunes $\Omega_{T,k}$ on the adaption dataset $\mathbb{D}_{Ad}(k)$ via G_{Ad} steps of gradient descents. The optimization objective is the loss function on the $\mathbb{D}_{Ad}(k)$, i.e., $\text{Loss}_{\mathbb{D}_{Ad}(k)}(\Omega_{T,k})$. Therefore, the parameter $\Omega_{T,k}$ can be updated by

$$\Omega_{T,k} \leftarrow \Omega_{T,k} - \beta \nabla_{\Omega_{T,k}} \text{Loss}_{\mathbb{D}_{Ad}(k)}(\Omega_{T,k}). \quad (12)$$

After the fine-tuning finished, the target-task-specific parameter $\Omega_{T,k}$ will be fixed. Let $\text{NMSE}_{Mt}(k)$ represent the NMSE of the meta-learning algorithm evaluated on the k -th target environment that can be obtained by testing the network on the dataset $\mathbb{D}_{Te}(k)$ using Eqs. (7) and (10). Then, the prediction NMSE of the meta-learning algorithm can be obtained by $\text{NMSE}_{Mt} = \sum_{k=1}^{K_T} \text{NMSE}_{Mt}(k) / K_T$. The concrete steps of the meta-learning algorithm are given in **Algorithm 3**.

Remark 3: The proposed meta-learning algorithm is inspired by the MAML algorithm in [34]. While it should be mentioned that several modifications have been made in the proposed meta-learning algorithm:

- i) The inner-task update only involves one step of gradient descent in [34] while the proposed algorithm adopts G_{Tr} steps to obtain better performance;
- ii) The across-task update is preformed by the stochastic gradient descent (SGD) algorithm in [34] while the proposed

Algorithm 3: Meta-learning algorithm for downlink CSI prediction

Input: Source tasks: $\{\mathcal{T}_S(k)\}_{k=1}^{K_S}$, Target tasks: $\{\mathcal{T}_T(k)\}_{k=1}^{K_T}$, inner-task learning rate: β , across-task learning rate: γ , number of gradsteps for inner-task training: G_{Tr} , number of tasks in each time step: K_B

Output: Meta-trained network parameter: Ω_{Mt} , Predicted downlink CSI based on $\{\mathbb{D}_{Te}(k)\}_{k=1}^{K_T}$, NMSE of the meta-learning algorithm: NMSE_{Mt}

- 1 Meta-training stage
- 2 Randomly initialize the network parameters Ω
- 3 **for** $t = 1, \dots$ **do**
- 4 Randomly select K_B tasks from $\{\mathcal{T}_S(k)\}_{k=1}^{K_S}$
- 5 Generate corresponding datasets $\{\mathbb{D}_{TrSup}(k)\}_{k=1}^{K_B}$ and $\{\mathbb{D}_{TrQue}(k)\}_{k=1}^{K_B}$
- 6 **for** $k = 1, \dots, K_B$ **do**
- 7 Initialize the parameter $\Omega_{S,k} \leftarrow \Omega$
- 8 **for** $g = 1, \dots, G_{Tr}$ **do**
- 9 Update $\Omega_{S,k}$ using Eq. (11)
- 10 **end**
- 11 Update Ω by using ADAM (learning rate γ) to minimize $\sum_{k=1}^{K_B} \text{Loss}_{\mathbb{D}_{TrQue}(k)}(\Omega_{S,k})$
- 12 **end**
- 13 **end**
- 14 Meta-trained network parameter: $\Omega_{Mt} \leftarrow \Omega$
- 15 Meta-adaption and Testing
- 16 Initialize NMSE: $\text{NMSE}_{Mt} \leftarrow 0$
- 17 **for** $k = 1, \dots, K_T$ **do**
- 18 Generate the datasets $\mathbb{D}_{Ad}(k)$ and $\mathbb{D}_{Te}(k)$ for $\mathcal{T}_T(k)$
- 19 Meta-adaption stage
- 20 Load the network parameter $\Omega_{T,k} \leftarrow \Omega_{Mt}$
- 21 **for** $g = 1, \dots, G_{Ad}$ **do**
- 22 Update $\Omega_{T,k}$ using Eq. (12)
- 23 **end**
- 24 Testing stage
- 25 Predict the downlink CSI base on $\mathbb{D}_{Te}(k)$ and $\Omega_{T,k}$ using Eq. (7)
- 26 Calculate $\text{NMSE}_{Mt}(k)$ using Eq. (10)
- 27 $\text{NMSE}_{Mt} \leftarrow \text{NMSE}_{Mt} + \text{NMSE}_{Mt}(k) / K_T$
- 28 **end**

algorithm adopts the ADAM algorithm instead of the SGD algorithm. This is because that the ADAM benefits from the moment technique and the parameter-specific learning rates, and thus outperforms SGD in many situations [44].

Fig. 4 illustrates the trajectories of parameter updating during the meta-training and meta-adaption stages of the meta-learning algorithm. The black solid line represents the updating trajectory of the network parameter Ω during the meta-training stage. The blue dashed lines represent the updating trajectories of the target-task-specific parameters $\{\Omega_{T,k}\}_{k=1}^3$ during the meta-adaption stage. The green dotted lines represent the trajectories of the source-task-specific parameters $\{\Omega_{S,k}\}_{k=1}^6$ during the inner-task updates. As shown in Fig. 4, K_B red

dash-dotted lines point to the next position of parameter Ω , which implies that K_B trained source-task-specific parameters are involved in the across-task update to determine the updating direction of Ω . As depicted in Fig. 3 and Fig. 4, the meta-learning algorithm takes the unique features of different tasks into account and exploits the joint guidance of multiple source tasks while the direct-transfer algorithm simply regards all the source tasks as one source task and ignores the structure information in different tasks.

D. Theoretical Analysis of the Meta-learning Algorithm

To understand why the meta-learning algorithm outperforms the direct-transfer algorithm, we focus on the loss function that is used to guide the updates of Ω for the meta-learning algorithm, i.e., $\sum_{k=1}^{K_B} \text{Loss}_{\mathbb{D}_{\text{TrQue}}(k)}(\Omega_{S,k})$. We add the superscript (t) to distinguish the parameters at different time steps and set G_{Tr} as 1 to simplify the parameter updates in the meta-training stage. Based on **Algorithm 3**, the loss function at the t -th time step is computed as

$$\begin{aligned} & \sum_{k=1}^{K_B} \text{Loss}_{\mathbb{D}_{\text{TrQue}}(k)}(\Omega_{S,k}^{(t)}) \quad (13a) \\ = & \sum_{k=1}^{K_B} \text{Loss}_{\mathbb{D}_{\text{TrQue}}(k)}(\Omega^{(t-1)} - \beta \nabla \text{Loss}_{\mathbb{D}_{\text{TrSup}}(k)}(\Omega^{(t-1)})) \\ \approx & \sum_{k=1}^{K_B} \text{Loss}_{\mathbb{D}_{\text{TrQue}}(k)}(\Omega^{(t-1)}) \\ & - \sum_{k=1}^{K_B} \beta \nabla \text{Loss}_{\mathbb{D}_{\text{TrSup}}(k)}(\Omega^{(t-1)}) \nabla \text{Loss}_{\mathbb{D}_{\text{TrQue}}(k)}(\Omega^{(t-1)}), \quad (13b) \end{aligned}$$

where Eq. (13b) is obtained based on the first-order Taylor expansion. The first term in Eq. (13b) represents the sum of the losses on query datasets. The second term in Eq. (13b) represents the sum of the negative inner products of the gradients on the query and the support datasets. We know that if the directions of the two gradients are closer, then the negative inner product will be smaller, which indicates that during the meta-training stage, the algorithm tries to maximize the similarity between the gradients on the query and the support datasets. Compared with the no-transfer and the direct-transfer algorithms, the meta-learning algorithm enhances the generalization capability between the query and the support datasets (also between the adaption and testing datasets), and therefore can adapt to a new task more effectively [45].

VI. SIMULATION RESULTS

In this section, we will first present the simulation scenario and default algorithm parameters. Then, the performance of the no-transfer, the direct-transfer, and the meta-learning algorithms will be evaluated and analyzed.

A. Simulation Setup

In the simulations, we consider the outdoor massive MIMO scenario that is constructed based on the accurate 3D ray-tracing simulator [46]. The scenario comprises 4 BSs and

massive randomly distributed user antennas and each BS is equipped with 64 antennas. The scenario covers an area of 1500×1500 square metres. A partial view of the ray-tracing scenario is illustrated in Fig. 5. There are total 1300 environments randomly distributed in the outdoor massive MIMO scenario, where each environment contains multiple possible user locations as shown in the partial enlarged picture.

To generate the training dataset, the uplink frequency is randomly selected in $[1, 3]$ GHz. The frequency difference between the uplink and the downlink is 120 MHz. For each environment, the 3D ray-tracing simulator first generates the channels between the user antennas and the corresponding BS antennas⁶. Then, the uplink and downlink channels of U selected users are collected as the sample pairs for the corresponding environment⁷. After obtained the sample pairs for all the environments, we randomly select 1500 environments out as the source environments and the rest of them are used as the target environments. For each source task, N_{Tr} sample pairs of one source environment are randomly selected out as the training dataset. For each target task, N_{Ad} and N_{Te} sample pairs of one target environment are separately selected out as the adaption and the testing datasets. Since the perfect channels are not available in practical situation, unless otherwise specified, all the sample pairs in the datasets are estimated by the linear minimum-mean-squared-error (LMMSE) algorithm⁸ [48] when the signal-to-noise ratio (SNR) is 20 dB and the pilot length is 64. Therefore, the overhead for the dataset collection is the pilot length multiplied by twice the number of sample pairs in the datasets.

The meta-learning, the no-transfer and the direct-transfer algorithms are all implemented on one computer with one GPU. TensorFlow 1.4.0 is employed as the deep learning framework. Unless otherwise specified, the parameters of the no-transfer, the direct-transfer, and the meta-learning algorithms are given in Tab. I. The specific values of these parameters are basically selected by trails and errors such that these algorithms perform well. The FNN adopted in this work has two hidden layers, and each hidden layer has 128 neurons. The numbers of neurons in the input and the output layers are consistent with the lengths of input and output data vectors, respectively. The trainable parameters of FNN are randomly initialized as truncated normal variables⁹ with normalized

⁶For more details about how to generate channels, please refer to [47].

⁷Based on the theory of deep learning, we can improve the generalization capability of the network over the frequency ranges by increasing the randomly selected frequencies, or improve the generalization capability of the network over users' positions by increasing U .

⁸In this work, we do not compare the proposed DTL based algorithm with conventional channel estimation algorithms (e.g. least squares, LMMSE and etc [48]) since the conventional methods need prohibitively high overheads to achieve the online downlink training and uplink feedback. While the proposed DTL based algorithms require neither downlink training nor uplink feedback after the offline training and the adaption stages are finished, which is a significant advantage over the conventional methods. In fact, the best way for the applications of the DTL based algorithms is to serve as complementary approaches of the conventional methods. We can collect adaption data during the applications of the conventional methods and then switch to the DTL algorithms when the data collection and adaption are finished.

⁹The truncated normal distribution is a normal distribution bounded by two standard deviations from the mean.

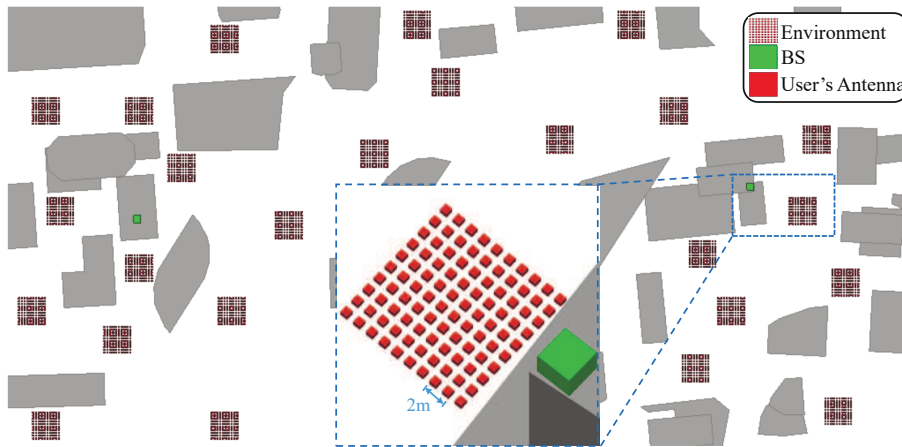


Fig. 5. A partial view of the ray-tracing scenario. The green little box represents the BS antennas. The red little box represents the user antennas in the same environments, where the distance between adjacent red little boxes is 2 m. This ray-tracing simulator shoots thousands of rays in all directions from the transmitter and records the strongest 25 paths that reach the receiver [46].

TABLE I
DEFAULT PARAMETERS FOR THE NO-TRANSFER, THE DIRECT-TRANSFER,
AND THE META-LEARNING ALGORITHMS

Parameter	Value
Learning rates: (γ, β)	(1e-3, 1e-6)
Exponential decay rates for ADAM: (ρ_1, ρ_2)	(0.9, 0.999)
Disturbance factor for ADAM: ϵ	1e-08
Number of source tasks: K_S	1500
Number of target tasks: K_T	800
Number of tasks in each training index: K_B	80
Number of samples in each source task: N_{Tr}	20
Number of samples in the target task: (N_{Ad}, N_{Te})	(20, 20)
Number of users in each task: U	25
Number of gradsteps: (G_{Tr}, G_{Ad})	(3, 1e3)
Batch size: V	128

variance¹⁰. To be fair, the number of training samples in \mathbb{D}_{STr} are equal to the number of training samples used in the meta-learning algorithm, i.e., $K_S \times N_{Tr}$. We use the average NMSE as the metric to evaluate the performance of algorithms, i.e., calculating the average NMSE of the prediction accuracy by repetitively (fine-tuning and then) testing 800 different target environments¹¹.

B. Complexity analysis

Tab. II compares the complexities of the no-transfer, the direct-transfer, and the meta-learning algorithms. In the training or adaption stages, the three algorithms repeat the following processes until the loss functions converge: 1) conduct forward propagation of the input and obtain the loss; 2) obtain the derivatives of the loss with respect to the network parameters; 3) update the network parameters. Since the derivative process requires much more time than the other two processes, we mainly focus on the complexities involved in derivatives. Based on [45], the meta-learning algorithm requires $(G_{Tr} + 1)$ -order derivatives, and therefore has a higher complexity than

¹⁰The weights of neurons in the l -th layer are initialized as truncated normal variables with variance $1/n_l$, where n_l is the number of neurons in the l -th layer.

¹¹The codes of this paper are available at [49].

the other two algorithms in the training stage. Tab. II displays the time required for the three algorithms to complete the training stage when G_{Tr} is 3. In the adaption stage, the meta-learning algorithm requires 1-order derivatives like the direct-transfer algorithm since across-task update is no longer needed. Tab. II shows the time required for the networks to adapt to a new environment when N_{Ad} is 20. It should be mentioned that once the adaption stage is finished, the network would be applicable for all users in the new environment. Given that the area for one environment is $20 \times 20 \text{ m}^2$ in our simulations, the proposed algorithms are not competitive for high-speed users (e.g., users with the movement speed higher than 40 m/s). It should be mentioned that the max speed of users can be increased by deploying a higher computational power hardware in BSs or selecting a larger learning rate for adaption. In the testing stage, the three algorithms only need to conduct a single-forward propagation of the input. Since the three algorithms all adopt the same FNN architecture, the total number of floating point operations for all the three algorithms is $\sum_{l=1}^L n_{l-1} n_l$. Tab. II displays the time required for the three algorithms to complete a single-forward propagation of one input vector.

C. Performance Evaluation

Fig. 6 depicts the NMSE performance of the no-transfer, the direct-transfer, and the meta-learning algorithms (i.e., $NMSE_{Nt}$, $NMSE_{Dt}$ and $NMSE_{Mt}$) versus the number of gradsteps G_{Ad} . Since the network parameters of the no-transfer algorithm do not fine-tune based on the target environment, the accuracy curve of the no-transfer algorithm is a horizontal line. As shown in Fig. 6, both the meta-learning and the direct-transfer algorithms are significantly better than the no-transfer algorithm, which indicates that additional samples for the target task and appropriate fine-tuning can improve the prediction accuracy, i.e., transfer learning is more suitable than classical deep learning in downlink channel prediction. Furthermore, the meta-learning algorithm outperforms the no-transfer and the direct-transfer algorithms, which demonstrates the superiority

TABLE II
COMPLEXITY ANALYSIS AND TIME COST FOR THE NO-TRANSFER, THE DIRECT-TRANSFER, AND THE META-LEARNING ALGORITHMS.

Algorithm	Training stage	adaption stage	testing stage
No-transfer	1-order (17.2 s)	-	$\sum_{l=1}^L n_{l-1} n_l$ (1.3e-6 s)
Direct-transfer	1-order (17.2 s)	1-order (0.25 s)	$\sum_{l=1}^L n_{l-1} n_l$ (1.3e-6 s)
Meta-learning	$(G_{Tr} + 1)$ -order (65.7 s)	1-order (0.24 s)	$\sum_{l=1}^L n_{l-1} n_l$ (1.3e-6 s)

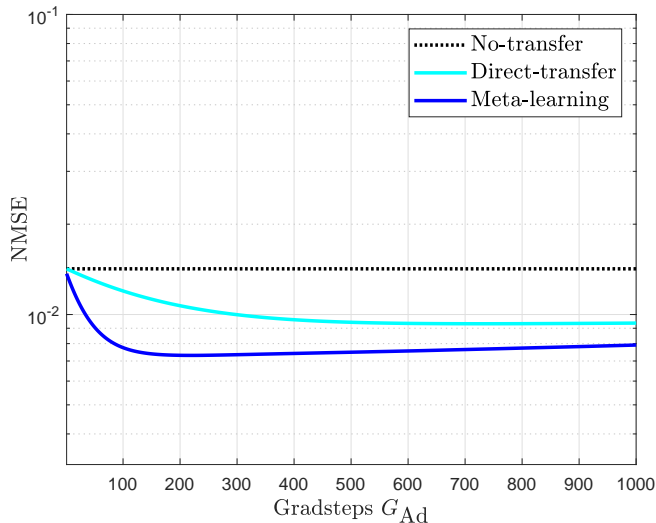


Fig. 6. The NMSE performance of the no-transfer, the direct-transfer, and

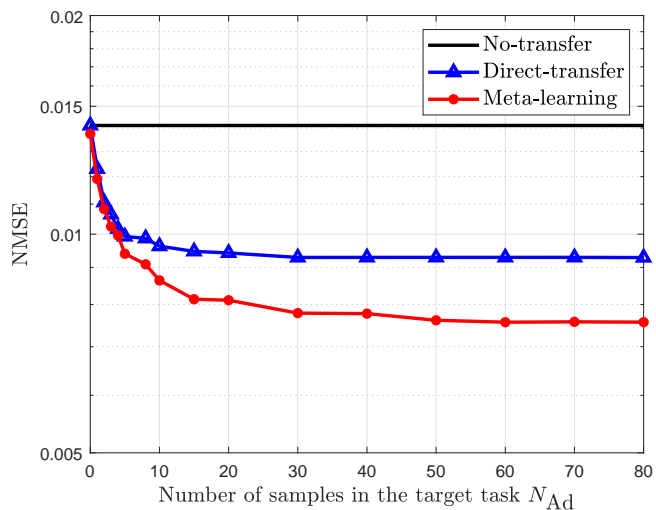


Fig. 7. The NMSE performance of the no-transfer, the direct-transfer, and the meta-learning algorithms versus the number of samples in \mathbb{D}_{AdSup} .

of the meta-learning algorithm. The performance of the meta-learning algorithm without meta-adaption stage is similar with the no-transfer algorithm, however, the NMSE of the meta-learning algorithm drops much faster than the no-transfer algorithm as the gradsteps G_{Ad} increases, which demonstrates that the meta-learning algorithm can find a better initialization for fast adaption than the direct-transfer algorithm. We have conducted extensive simulations to investigate the impacts of learning rate β on the performance of the direct-transfer and the meta-learning algorithms in the adaption stage. Sim-

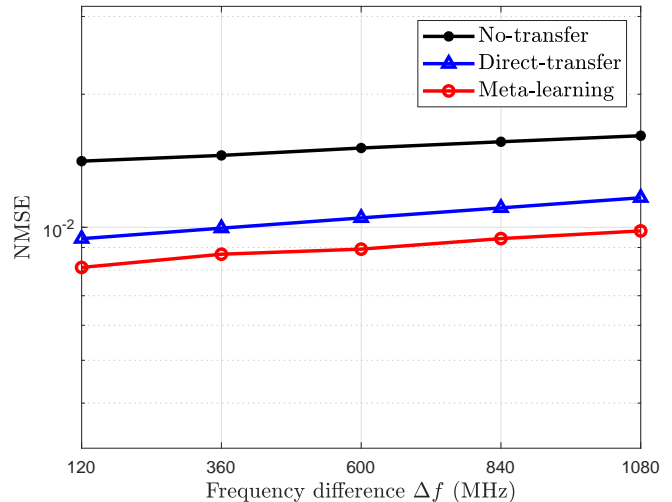


Fig. 8. The NMSE performance of the no-transfer, the direct-transfer, and the meta-learning algorithms versus the frequency difference Δf . The network

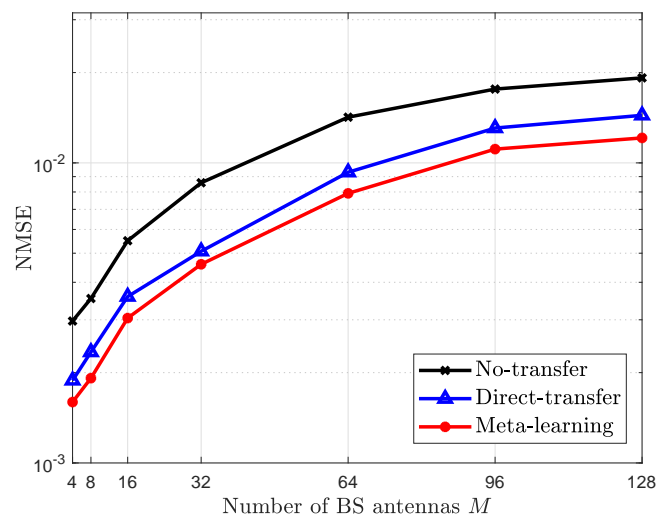


Fig. 9. The NMSE performance of the no-transfer, the direct-transfer, and the meta-learning algorithms versus the number of BS antennas M . The network is trained for each BS antenna number separately.

ulations show that a large learning rate can speed up the convergence but would cause oscillations and overfitting. In practical systems, we can select a larger learning rate for a faster convergence, select a smaller learning rate for a more stable convergence, or adaptively change the learning rate during the adaption stages to achieve a better balance. It should be emphasized that no matter what value β is, the meta-learning algorithm always achieves a better accuracy than the direct-transfer algorithm.

Fig. 7 depicts the NMSE performance of the no-transfer, the direct-transfer, and the meta-learning algorithms versus the number of samples in $\mathbb{D}_{\text{AdSup}}$. Since the network parameters of the no-transfer algorithm do not use the dataset $\mathbb{D}_{\text{AdSup}}$, the accuracy curve of the no-transfer algorithm is a horizontal line. As shown in Fig. 7, the meta-learning algorithm consistently outperforms the direct-transfer algorithm as the sample size increases, which validates its superiority in transfer learning. Moreover, the prediction accuracies of both the direct-transfer and the meta-learning algorithms improve as the sample size increases while the improvement rates of both algorithms decrease as the sample size increases. When the sample size is larger than 60, the performance of the direct-transfer and the meta-learning algorithms both become saturated, which indicates that a maximum of 60 channel samples in a new environment are required for the network to fully adapt to the new environment, i.e., to predict the downlink channels for any users in the new environment.

Fig. 8 shows the NMSE performance of the no-transfer, the direct-transfer, and the meta-learning algorithms versus the frequency difference Δf . The prediction accuracies of the three algorithms all degrade as the frequency difference increases. This is because the channel correlation between the uplink and the downlink tends to weaken as the frequency difference increases, and the degradation resulted from the frequency difference is not destructive for the uplink based downlink channel prediction. The remarkable robustness of DNNs over frequency difference validates the feasibility of channel or beam predictions across wide bandwidths [24].

Fig. 9 shows NMSE performance of the no-transfer, the direct-transfer, and the meta-learning algorithms versus the number of BS antennas M . For each antenna number point, the adopted FNN has the same hidden layers but different numbers of neurons in the input and the output layers to keep consistent with the lengths of the input and the output vectors. As shown in Fig. 9, the prediction accuracies of the three algorithms all degrade as the number of BS antennas increases. This involves a common phenomenon “dimensionality curse” [50], which refers the phenomenon that when the data dimensionality increases, the dimension of feature space increases so fast that the available data become sparse and dissimilar in many ways. In this case, the amount of data required to support the data analysis often grows exponentially with the dimensionality. Therefore, the performance of networks often degrades when the data dimensionality increases but the number of training samples does not increase accordingly. When the training dataset is limited, one feasible solution to improve the network performance is to reduce the lengths of the input and the output vectors. For example, [18] proposed to improve the network performance by dividing the input and the output vectors into multiple shorter vectors and then independently training a network for each of the shortened vector pairs.

Fig. 10 depicts the NMSE performance of the no-transfer, the direct-transfer, and the meta-learning algorithms versus the SNR in collecting adaption datasets. The performance of the direct-transfer and the meta-learning algorithms degrades as SNR decreases when SNR is lower than 0 dB. When SNR is lower than -40 dB, the adaption processes cannot improve

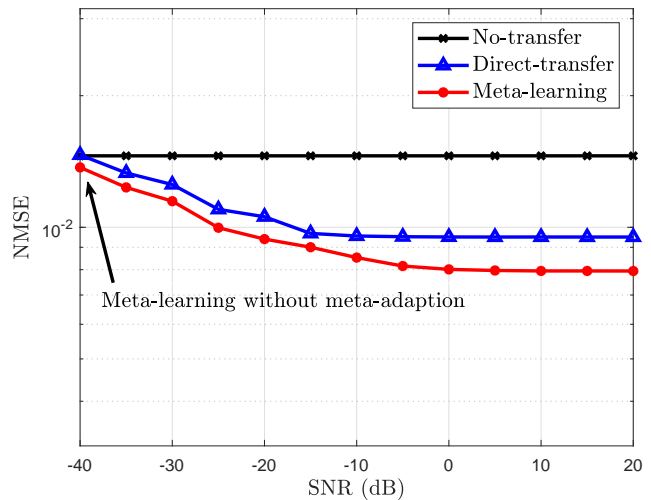


Fig. 10. The NMSE performance of the no-transfer, the direct-transfer, and the meta-learning algorithms versus the SNR in collecting adaption datasets.

the performance of the direct-transfer or the meta-learning algorithms.

VII. CONCLUSION

In this paper, we formulated the downlink channel prediction for FDD massive MIMO systems as a deep transfer learning problem, where each learning task represents the downlink CSI prediction from the uplink CSI for a certain environment. Then, we proposed the no-transfer, direct-transfer and meta-learning algorithms based on the fully-connected neural network architecture. The no-transfer algorithm trains the network in the classical deep learning manner. The direct-transfer algorithm fine-tunes the network based on the initialization of the no-transfer algorithm. The meta-learning algorithm learns a model initialization that can effectively adapt to a new environment with a small amount of labeled data. Simulation results have shown that the proposed meta-learning algorithm significantly outperforms the direct-transfer and the no-transfer algorithms, which demonstrates its effectiveness and superiority.

REFERENCES

- [1] B. Wang, F. Gao, S. Jin, H. Lin, and G. Y. Li, “Spatial- and frequency-wideband effects in millimeter-wave massive MIMO systems,” *IEEE Trans. Signal Process.*, vol. 66, no. 13, pp. 3393–3406, Jul. 2018.
- [2] H. Xie, F. Gao, S. Zhang, and S. Jin, “A unified transmission strategy for TDD/FDD massive MIMO systems with spatial basis expansion model,” *IEEE Trans. Vehicular Technol.*, vol. 66, no. 4, pp. 3170–3184, Apr. 2017.
- [3] B. Wang, F. Gao, S. Jin, H. Lin, G. Y. Li, S. Sun, and T. S. Rappaport, “Spatial-wideband effect in massive MIMO with application in mmwave systems,” *IEEE Commun. Mag.*, vol. 56, no. 12, pp. 134–141, Dec. 2018.
- [4] J. Hoydis, C. Hoek, T. Wild, and S. ten Brink, “Channel measurements for large antenna arrays,” in *Proc. Int. Symp. Wireless Commun. Systems (ISWCS)*, Paris, France, Aug. 2012, pp. 811–815.
- [5] Y. Zhou, M. Herdin, A. Sayeed, and E. Bonek, “Experimental study of MIMO channel statistics and capacity via the virtual channel representation,” *Univ. Wisconsin-Madison, Madison, WI, USA, Tech. Rep.*, vol. 5, pp. 10–15, 2007.
- [6] K. Hugl, K. Kalliola, and J. Laurila, “Spatial reciprocity of uplink and downlink radio channels in FDD systems,” in *Proc. COST*. Citeseer, 2002, vol. 273, p. 066.

- [7] Y. Han, Q. Liu, C. Wen, S. Jin, and K. Wong, "FDD massive MIMO based on efficient downlink channel reconstruction," *IEEE Trans. Commun.*, vol. 67, no. 6, pp. 4020–4034, Jun. 2019.
- [8] H. Xie, F. Gao, S. Jin, J. Fang, and Y. Liang, "Channel estimation for TDD/FDD massive MIMO systems with channel covariance computing," *IEEE Trans. Wireless Commun.*, vol. 17, no. 6, pp. 4206–4218, Jun. 2018.
- [9] X. Rao and V. K. N. Lau, "Distributed compressive CSIT estimation and feedback for FDD multi-user massive MIMO systems," *IEEE Trans. Signal Process.*, vol. 62, no. 12, pp. 3261–3271, Jun. 2014.
- [10] M. E. Eltayeb, T. Y. Al-Naffouri, and H. R. Bahrami, "Compressive sensing for feedback reduction in MIMO broadcast channels," *IEEE Trans. Commun.*, vol. 62, no. 9, pp. 3209–3222, Sep. 2014.
- [11] H. He, S. Jin, C. Wen, F. Gao, G. Y. Li, and Z. Xu, "Model-driven deep learning for physical layer communications," *IEEE Wireless Commun.*, vol. 26, no. 5, pp. 77–83, Oct. 2019.
- [12] Z. Qin, H. Ye, G. Y. Li, and B. F. Juang, "Deep learning in physical layer communications," *IEEE Wireless Commun.*, vol. 26, no. 2, pp. 93–99, Apr. 2019.
- [13] Y. Yang, F. Gao, X. Ma, and S. Zhang, "Deep learning-based channel estimation for doubly selective fading channels," *IEEE Access*, vol. 7, pp. 36579–36589, Mar. 2019.
- [14] H. He, C. Wen, S. Jin, and G. Y. Li, "Deep learning-based channel estimation for beamspace mmwave massive MIMO systems," *IEEE Wireless Commun. Lett.*, vol. 7, no. 5, pp. 852–855, Oct. 2018.
- [15] S. Gao, P. Dong, Z. Pan, and G. Y. Li, "Deep learning based channel estimation for massive MIMO with mixed-resolution ADCs," *IEEE Commun. Lett.*, vol. 23, no. 11, pp. 1989–1993, Nov. 2019.
- [16] P. Dong, H. Zhang, G. Y. Li, I. S. Gaspar, and N. NaderiAlizadeh, "Deep CNN-based channel estimation for mmwave massive MIMO systems," *IEEE J. Sel. Topics Signal Process.*, vol. 13, no. 5, pp. 989–1000, Sept. 2019.
- [17] Z. Jia, W. Cheng, and H. Zhang, "A partial learning-based detection scheme for massive MIMO," *IEEE Wireless Commun. Lett.*, vol. 8, no. 4, pp. 1137–1140, Aug. 2019.
- [18] H. Ye, G. Y. Li, and B. Juang, "Power of deep learning for channel estimation and signal detection in OFDM systems," *IEEE Wireless Commun. Lett.*, vol. 7, no. 1, pp. 114–117, Feb. 2018.
- [19] C. Wen, W. Shih, and S. Jin, "Deep learning for massive MIMO CSI feedback," *IEEE Wireless Commun. Lett.*, vol. 7, no. 5, pp. 748–751, Oct. 2018.
- [20] T. Wang, C. Wen, S. Jin, and G. Y. Li, "Deep learning-based CSI feedback approach for time-varying massive MIMO channels," *IEEE Wireless Commun. Lett.*, vol. 8, no. 2, pp. 416–419, Apr. 2019.
- [21] J. Guo, C. Wen, S. Jin, and G. Y. Li, "Convolutional neural network based multiple-rate compressive sensing for massive MIMO CSI feedback: Design, simulation, and analysis," *IEEE Trans. Wireless Commun.*, vol. 19, no. 4, pp. 2827–2840, Apr. 2020.
- [22] W. Xu, F. Gao, S. Jin, and A. Alkhateeb, "3D scene based beam selection for mmwave communications," *arXiv preprint arXiv:1911.08409*, 2019.
- [23] M. Alrabeiah, A. Hredzak, Z. Liu, and A. Alkhateeb, "ViWi: A deep learning dataset framework for vision-aided wireless communications," *arXiv preprint arXiv:1911.06257*, 2019.
- [24] M. Alrabeiah and A. Alkhateeb, "Deep learning for mmwave beam and blockage prediction using sub-6GHz channels," *arXiv preprint arXiv:1910.02900*, 2019.
- [25] X. Li and A. Alkhateeb, "Deep learning for direct hybrid precoding in millimeter wave massive MIMO systems," in *53rd Asilomar Conf. Signals, Systems, Computers*, California, USA, Nov. 2019, pp. 800–805.
- [26] Y. Yang, F. Gao, C. Qian, and G. Liao, "Model-aided deep neural network for source number detection," *IEEE Signal Process. Lett.*, vol. 27, pp. 91–95, 2020.
- [27] M. S. Safari, V. Pourahmadi, and S. Sodagari, "Deep UL2DL: Data-driven channel knowledge transfer from uplink to downlink," *IEEE Open J. Vehicular Technol.*, vol. 1, pp. 29–44, Dec. 2020.
- [28] P. Dong, H. Zhang, and G. Y. Li, "Machine learning prediction based CSI acquisition for FDD massive MIMO downlink," in *Proc. IEEE Global Commun. Conf. (GLOBECOM)*, Abu Dhabi, United Arab Emirates, Dec. 2018, pp. 1–6.
- [29] M. Alrabeiah and A. Alkhateeb, "Deep learning for TDD and FDD massive MIMO: Mapping channels in space and frequency," in *Proc. 53rd Asilomar Conf. Signals, Systems, Computers*, California, USA, 2019, pp. 1465–1470.
- [30] Y. Yang, F. Gao, G. Y. Li, and M. Jian, "Deep learning based downlink channel prediction for FDD massive MIMO system," *IEEE Commun. Lett.*, vol. 23, no. 11, pp. 1994–1998, Nov. 2019.
- [31] S. J. Pan and Q. Yang, "A survey on transfer learning," *IEEE Trans. Knowledge and Data Engineering*, vol. 22, no. 10, pp. 1345–1359, Oct. 2010.
- [32] J. Lin, Y. Wang, Y. Xia, T. He, and Z. Chen, "Learning to transfer: Unsupervised meta domain translation," *arXiv preprint arXiv:1906.00181*, 2019.
- [33] C. Tan, F. Sun, T. Kong, W. Zhang, C. Yang, and C. Liu, "A survey on deep transfer learning," in *Proc. Int. Conf. Artificial Neural Networks*. Springer, 2018, pp. 270–279.
- [34] C. Finn, P. Abbeel, and S. Levine, "Model-agnostic meta-learning for fast adaptation of deep networks," in *Proc. 34th Int. Conf. Machine Learning*. JMLR. org, 2017, vol. 70, pp. 1126–1135.
- [35] M. Andrychowicz, M. Denil, S. Colmenarejo, M. W. Hoffman, D. Pfau, T. Schaul, B. Shillingford, and N. de Freitas, "Learning to learn by gradient descent by gradient descent," in *Proc. 30th Int. Conf. Neural Inf. Process. Systems*, Barcelona, Spain, 2016, pp. 3988–3996.
- [36] A. Santoro, S. Bartunov, M. Botvinick, D. Wierstra, and T. Lillicrap, "Meta-learning with memory-augmented neural networks," in *Proc. Int. Conf. machine learning (ICML)*, 2016, pp. 1842–1850.
- [37] S. Ravi and H. Larochelle, "Optimization as a model for few-shot learning," in *Proc. Int. Conf. Learning Representations (ICLR)*, Toulon, France, 2017.
- [38] L. Liu and W. Yu, "Massive connectivity with massive MIMO part i: Device activity detection and channel estimation," *IEEE Tran. Signal Process.*, vol. 66, no. 11, pp. 2933–2946, Jun. 2018.
- [39] K. Hornik, M. Stinchcombe, and H. White, "Multilayer feedforward networks are universal approximators," *Neural netw.*, vol. 2, no. 5, pp. 359–366, 1989.
- [40] D. Kingma and J. Ba, "Adam: A method for stochastic optimization," *arXiv preprint arXiv:1412.6980*, 2014.
- [41] I. Goodfellow, Y. Bengio, and A. Courville, *Deep Learning*, MIT Press, 2016, <http://www.deeplearningbook.org>.
- [42] S. Liang, R. Sun, Y. Li, and R. Srikant, "Understanding the loss surface of neural networks for binary classification," *arXiv preprint arXiv:1803.00909*, 2018.
- [43] I. Sutskever, J. Martens, G. Dahl, and G. Hinton, "On the importance of initialization and momentum in deep learning," in *Proc. Int. Conf. Machine Learning (ICML)*, Atlanta, USA, 2013, pp. 1139–1147.
- [44] J. Chen and A. Kyrillidis, "Decaying momentum helps neural network training," *arXiv preprint arXiv:1910.04952*, 2019.
- [45] A. Nichol, J. Achiam, and J. Schulman, "On first-order meta-learning algorithms," *arXiv preprint arXiv:1803.02999*, Aug. 2018.
- [46] "Remcom wireless insite," <https://www.remcom.com/wireless-insite-em-propagation-software>.
- [47] A. Alkhateeb, "DeepMIMO: A generic deep learning dataset for millimeter wave and massive MIMO applications," in *Proc. Inf. Theory and Applications Workshop (ITA)*, San Diego, CA, Feb. 2019, pp. 1–8.
- [48] M. Biguesh and A. B. Gershman, "Training-based MIMO channel estimation: a study of estimator tradeoffs and optimal training signals," *IEEE Trans. Signal Process.*, vol. 54, no. 3, pp. 884–893, Mar. 2006.
- [49] "Codes," [Online]. Available: <https://github.com/yangyuwenyang/Codes-for-Deep-Trans>
- [50] R. Bellman, "Dynamic programming," *Science*, vol. 153, no. 3731, pp. 34–37, 1966.